INTERNATIONAL JOURNAL OF CLIMATOLOGY
Int. J. Climatol. **19**: 1535–1560 (1999)

NORTHERN HEMISPHERE SNOW EXTENT: REGIONAL VARIABILITY 1972–1994

ALLAN FREI[a,*] and DAVID A. ROBINSON[b]
[a] *CIRES/NSIDC, University of Colorado, Campus Box 449, Boulder, CO 80309, USA*
[b] *Rutgers University, Department of Geography, New Brunswick, NJ 08903, USA*

Received 7 August 1997
Revised 11 March 1999
Accepted 13 March 1999

ABSTRACT

Snow cover is an important hydrologic and climatic variable due to its effects on water supplies, and on energy and mass exchanges at the surface. We investigate the kinematics and climatology of Northern Hemisphere snow extent between 1972 and 1994, and associated circulation patterns. Interannual fluctuations of North American and Eurasian snow extents are driven by both hemispheric scale signals, as well as signals from smaller 'coherent' regions, within which interannual fluctuations of snow extent are highly correlated. These regions cover only 2–6% of the continental land area north of 20°N, yet during many months they explain more than 60% of the variance in continental snow extent. They are identified using Principal Components Analysis (PCA) of digitized snow extent charts obtained from the National Oceanic and Atmospheric Administration (NOAA). Significant month-to-month persistence is found over western North America and Europe during winter and spring. Geographically and seasonally dependent associations are identified between North American snow extent and atmospheric circulation patterns, surface air temperature, and snowfall. Over western North America, snow extent is associated with the longitudinal position of the North American ridge. Over eastern North America, snow extent is associated with a meridional oscillation in the 500-mb geopotential height field. These teleconnection patterns, derived using composite analyses, are associated with secondary modes of tropospheric variability during autumn and winter. During spring, snow extent becomes effectively decoupled from tropospheric dynamics. These results are useful for understanding the natural variability of the climate system, reconstructing pre-satellite era climate variability, evaluating climate models, and detecting climate change.

KEY WORDS: snow; Northern Hemisphere; principal components analysis; climate variability

1. INTRODUCTION AND LITERATURE REVIEW

Snow cover is an important climatic and hydrologic variable. In many areas it is a critical source of drinking water. Steppuhn (1981) estimates that snow accounts for at least one-third of all irrigation water in the world. Due to its impact on energy and mass exchanges at the surface, snow cover affects global and regional radiative and thermal energy budgets, air mass formation, weather systems, and thermal regimes in underlying soil and permafrost (Berry, 1981; Barry, 1985; Shine *et al.*, 1990).

Seasonal and interannual variations of snow extent across the Northern Hemisphere have been derived in a consistent manner from visible satellite imagery produced by the National Oceanic and Atmospheric Administration (NOAA) since the early 1970s (Dewey and Heim, 1982; Matson *et al.*, 1986; Wiesnet *et al.*, 1987; Masuda *et al.*, 1993; Robinson, 1993b). Since the late 1970s, passive microwave brightness temperatures have also been used to estimate hemispheric scale snow extent and snow/water-equivalent (Chang *et al.*, 1990), but estimates of extent are generally less accurate than visible values due to microwave difficulties in detecting shallow, patchy, or wet snow; snow in vegetated or forested areas; and snow lying over unfrozen ground (Robinson 1993a). The geographic extent of snow cover over Northern

* Correspondence to: CIRES/NSIDC, University of Colorado, Campus Box 449, Boulder, CO 80309, USA.Tel.: +1 303 4926085; fax: +1 303 4922468; e-mail: frei@kryos.colorado.edu

CCC 0899–8418/99/141535–26$17.50

Hemisphere lands varies seasonally, reaching a maximum of approximately 46×10^6 km^2 in January and February, and a minimum of about 4×10^6 km^2 in August. Between 60% and 65% of winter snow cover is found over Eurasia, and most mid-summer snow cover is over Greenland. Interannual fluctuations, though much smaller than seasonal ones, are sufficiently large to have substantial impacts on regional hydrology and radiative regimes.

In the first portion of this analysis, regions in the Northern Hemisphere over which snow cover fluctuates in a coherent manner are identified. Several earlier reports have examined the spatial scale at which interannual variations of snow extent occur (Gutzler and Rosen, 1992; Robinson *et al*., 1995). They found that less than 40% of observed interannual snow cover fluctuations are explained by continental to hemispheric scale forcing. In those studies, regions were defined *a priori*, and not directly from snow cover observations. In other investigations, multivariate techniques have been employed to reduce large data sets, and to identify regional characteristics of snow cover fluctuations directly from observations (Iwasaki, 1991; Brown, 1995, 1997). Leathers *et al*., (1993) applied similar techniques to snow*fall* data, identifying regions of coherent snowfall that do not directly correspond to regions derived from snow *extent* observations. In the report presented here, multivariate techniques are applied to monthly observations of Northern Hemisphere snow extent from September through June. Regional snow extent fluctuations between 1972 and 1994 are analysed, and interactions between regional and continental scale fluctuations are quantified.

In the second portion of this study, circulation patterns associated with snow extent over North American regions are examined. Numerous empirical and modelling studies have examined the relationship between snow cover and one or more other variables such as surface air temperature, precipitation, storm tracks, and tropospheric geopotential heights. These studies focused on a variety of spatial scales, including local studies from individual meteorological stations (Wagner, 1973; Baker *et al*., 1992), regional studies over areas such as the eastern US (Dickson and Namias, 1976; Dewey, 1977; van Loon and Rogers, 1978; Namias, 1985; Ross and Walsh, 1986; Leathers *et al*., 1995; Serreze *et al*., 1998; Clark and Serreze, 1999b), continental scale studies over North America or Eurasia (Walsh *et al*., 1982, 1985; Heim and Dewey, 1984; Cerveny and Balling, 1992; Karl *et al*., 1993; Leathers *et al*., 1995; Robinson and Leathers, 1993; Leathers and Robinson, 1993, 1997; Clark *et al*., 1999; Clark and Serreze, 1999a) as well as studies covering the entire Northern Hemisphere (Foster *et al*., 1983; Robinson *et al*., 1991; Groisman *et al*., 1994a,b; Clark, 1998). Several researchers have identified links between Eurasian snow cover during the winter, spring, and summer seasons to the summer monsoon over southeast Asia (Hahn and Shukla, 1976; Dey and Bhanu Kumar, 1983; Dey *et al*., 1985; Barnett *et al*., 1989; Sankar-Rao *et al*., 1996; Yang, 1996).

Many studies show that the influence of snow on the surface energy budget causes a feedback effect on tropospheric temperatures as well as dynamics. Foster *et al*. (1983) found that winter snow extent and mid-continental temperatures are highly correlated over North America, while over Eurasia snow extent during autumn is correlated to mid-continental winter air temperatures. Ross and Walsh (1986) identified the feedback effect of snow on surface air temperatures over the eastern US, whereby enhanced baroclinicity at the snow margin, especially along the coast, contributed to the intensification and steering of storms during high snow years. Leathers *et al*. (1995) found that snow over the north-eastern US can depress daily maximum and minimum temperatures by 5–6°C. Cold surface temperatures centred over the south-eastern US, and above-average snowfall over the north-eastern US, act to prolong and reinforce climatic regimes over Greenland, and, via teleconnections, elsewhere in the Northern Hemisphere (i.e., Europe, the Mediterranean Sea) (Dickson and Namias, 1976; van Loon and Rogers, 1978).

We also investigate associations between tropospheric teleconnection patterns and snow extent over North America. The Pacific–North American (PNA) oscillation, an important mode of atmospheric variability over North America during winter, has been analysed extensively (Wallace and Gutzler, 1981; Barnston and Livezey, 1987; Leathers *et al*., 1991; Leathers and Palecki, 1992). (Literature reviews can be found in Wallace and Gutzler, 1981 and Leathers *et al*., 1991.) The North Atlantic Oscillation (NAO), a dipole or seesaw pattern over the North Atlantic Ocean, is also a primary mode of atmospheric circulation (Horel, 1981; Wallace and Gutzler, 1981; Barnston and Livezey, 1987). Gutzler and Rosen

(1992) found a significant relationship between the PNA and western snow extent during December and January, and a significant correlation between the NAO and eastern snow extent during February, but not during December or January. Walsh (1995) observed that the record of sea-ice extent in eastern Canada resembles an NAO signal. Serreze *et al.* (1998) and Clark and Serreze (1999b) observed areas where *snowfall* is affected by the PNA oscillation. Here, we derive for the first time teleconnection indices over the North American sector directly from snow observations. These patterns resemble, but are not identical to, the PNA and NAO patterns.

The observational data sets used in this report are presented in the second section. The third section shows the methodology for the regional analysis, as well as the comprehensive sensitivity analysis for the number of components retained for rotation in the Principal Component Analyses (PCA). In the fourth section we report the results of the regional analysis. The fifth and sixth sections show the methodology and results, respectively, of the circulation analysis. Readers not interested in details of the methodologies and sensitivity tests can skip to the third and fifth sections. The paper concludes with a summary and conclusions in the seventh section. In a companion paper (Frei *et al.*, 1999), these results are used to reconstruct North American snow extent back to the early 20th century.

2. OBSERVATIONAL DATA

2.1. Snow observations

Charts of Northern Hemisphere snow cover extent, produced by NOAA, from January 1972 through December 1994, are used in this analysis. These weekly charts are derived from visual interpretation of photographic copies of visible-band satellite images by trained meteorologists. Limitations of visible imagery for snow cover detection include problems with low solar illumination, cloudiness, dense forest cover, and sub-grid resolution snow features (e.g., in areas of steep terrain). However, at a monthly resolution these data are suitable for climatic studies (Kukla and Robinson, 1981; Wiesnet *et al.*, 1987).

The images are digitized using the National Meteorological Center Limited-Area Fine Mesh Grid, an 89×89 cell cartesian grid placed over a Northern Hemisphere polar projection. This grid includes more than 5000 cells over land, with resolutions between 16000 km^2 and 42000 km^2. For each week, if a cell is interpreted to be at least 50% snow covered, it is considered snow covered; otherwise it is considered snow free. Weekly charts identify snow in a grid cell on the latest day of the week during which the ground was visible. Robinson (1993b) devised an improved routine to calculate monthly average snow frequencies from weekly charts, and applied corrections for inconsistencies in the demarcation of land versus ocean grid cells used in chart digitization. The data set used in this study contains monthly average snow cover frequencies for each grid cell for the 23 year period between 1972 and 1994.

Station observations of snow cover over the contiguous US are obtained from the Historical Daily Climate Dataset (HDCD) (Robinson, 1993c). The HDCD contains long-term digitized records of daily snow depth, snowfall, precipitation, maximum and minimum temperatures from over 1100 cooperative climate stations. All data are quality controlled and checked for inconsistencies, errors, and missing values. In this study, data between 1972 and 1993 are used to calculate regional average temperature and precipitation during the satellite-era.

2.2. Other data sources

Monthly mean 500-mb geopotential heights over North America, from 30°N to 80°N, and from 180°W to 20°W longitude, are obtained from the National Meteorological Center (NMC) (recently renamed the National Center for Environmental Prediction) on a 2.5° latitude $\times$ 2.5° longitude grid. Twice daily since 1957, 500-mb height observations have been taken at 00:00 and 12:00 UTC. Monthly mean values are obtained from averages of the two daily values.

To examine daily weather patterns, Daily Weather Maps from the US Department of Commerce are used. Information on surface cyclones and storm tracks is derived from the NMC octagonal grid of

twice-daily sea level pressure arrays using the algorithm of Serreze *et al.* (1996). All surface lows with closed contours (i.e., grid points with surface pressure at least 2-mb lower than all surrounding grid points) are considered cyclones.

3. METHODOLOGY FOR REGIONAL ANALYSIS

The NOAA data set is analysed to determine whether a significant portion of the variance in Northern Hemisphere snow extent can be explained by regional signals, and, if so, to examine interannual fluctuations of snow extent within those regions. The first step is to identify geographic areas on each continent over which snow extent is ephemeral during each month ('active areas'). Second, PCA are performed for each month to identify regions within which snow cover fluctuations are temporally correlated ('coherent regions'). Spatial and temporal variations of snow in these regions are examined. Third, linear multiple regression and correlation analyses are employed to explore interactions of snow variability between regional and continental scales. Results from these three portions of the analyses are presented in the fourth section (a through c). At each step we attempt to ensure that the procedure provides robust results.

3.1. (a) Method for selecting active areas

In step one, for each month from September through June, only those grid cells over land with snow cover frequencies between 10% and 90% for $X \geq 33\%$ of the time (i.e. at least 8 of 23 years) are chosen for further analysis. These regions are called areas of 'active snow fluctuation', and exclude grid cells that are usually snow covered or snow free. For most months, this reduces the data set from several thousand to several hundred grid cells, covering between 10% and 29% of the Northern Hemisphere land area north of 20°N. Other investigators have defined areas of transient snow extent similarly, but on time scales of 2 or more months (Karl *et al.*, 1993; Groisman *et al.*, 1994b). We find that the monthly time scale is appropriate for two reasons. First, the areas of active snow fluctuation change each month during spring and autumn. Second, even during winter (December through March), when month-to-month changes in active areas are relatively small, the regions of coherent snow fluctuations found within the active areas vary.

3.1.1. Method for testing stability of active grid cell criterion. Sensitivity tests are performed to ensure that the method for choosing grid cells to be included in the active area provides robust results. For a selection of 3 months, we examine solutions with X (see previous paragraph for definition) at 10%, 25%, and 33% (smaller X values include more grid cells in the active area). In addition, for each X value chosen, we remove random selections of up to 15% of the grid cells. For each test case, the identical PCA procedure is applied, and eight components are retained for rotation. We find that the $X = 10\%$ solutions differ even in some of the larger regions, the $X = 25\%$ regions differ only in the smaller regions, and the $X = 33\%$ regions are robust except for one small region in 1 month. Thus, we choose to define the active area using $X = 33\%$.

3.2. (b) Method for PCA

For each month, a PCA with a Varimax rotation is applied to all cells within the active area across the Northern Hemisphere. Although the resulting correlation matrix has a high ratio of variables to cases, this is common in climatological studies (e.g., Barnston and Livezey, 1987) since long time series are often unavailable. The Varimax transformation has a number of properties that are advantageous (Horel, 1981): it increases discrimination among the loadings, making them easier to interpret; it is independent of the spatial domain, so that a rotated PCA including only North American grid cells yields identical regions to a rotated PCA including all Northern Hemisphere grid cells; and it

maintains the orthogonality of the score time series, a property which we exploit in subsequent regression analyses. Extensive tests for the sensitivity of the solution to the number of components retained for rotation are reported in the third section (part d).

3.2.1. Method for defining coherent regions. We define the boundaries of 'coherent' regions to facilitate calculation of regional temperatures and snowfall using station-based observations. Only those components that explain $\geq 50\%$ of the variance (component loading ≥ 0.71) of at least three adjacent grid cells are retained for further analysis. Using this criterion, coherent regions do not overlap geographically; all grid cells within coherent regions have $\geq 50\%$ of their variance explained by one common time series (the score time series); and, ground-based observations can be regionally-averaged in a clear and consistent manner by using stations that are located within the spatial domain of each coherent region. Thus, unlike typical applications of PCA, in this analysis the spatial characteristics of the regions, rather than the amount of explained variance, are the primary criteria choosing which components to retain for further analysis.

3.3. (c) Method for exploring regional–continental scale interactions

To quantify interactions between regional and continental scale fluctuations, a least squares linear multiple regression analysis is performed for each month over each continent. The predictand is continental (either North American or Eurasian) snow cover extent derived from the NOAA digitized data set. The predictors are score time series of snow extent in each coherent region from the appropriate continent. Predictors are orthogonal, simplifying the interpretation of regression results. Cross-validated (CV) correlation coefficients (Livezey, 1995) are used to minimize the bias in estimates of regression skill. In this technique, for each regression the coefficients are calculated n times ($n =$ # years in regression), each time removing one point (i.e. year) from the model. Thus, the predicted value for each time point is calculated from a regression equation using the $(n-1)$ *other* time points. Then, the cross-validated percent of variance explained $(x-r^2)$ is calculated using cross-validated predicted values.

3.4. (d) Sensitivity tests for rotated PCA solutions

We examine the sensitivity of results to the number of components retained for rotation. Following O'Lenic and Livezey (1988), for each month the scree plot (eigenvalue versus component number) is examined to identify potential subsets of components to be retained (i.e. determining the lowest mode to be included in the rotation). These potential subsets are identified by points in the scree plot where the slope decreases, referred to as 'ends of shelves' by O'Lenic and Livezey. Then, the solutions for different subsets of rotated components are compared, and the solution deemed most appropriate for the problem at hand is identified. Solutions in which too many modes are retained may include higher frequency noise and lead to over-regionalization, while solutions with too few components may exclude important modes of variability and distort regional patterns. For our purposes, we require solutions in which the regional spatial patterns, as well as their associated time series, are robust. This method combines objective criteria for identifying potential solutions with more subjective criteria for choosing the most appropriate solution.

3.4.1. Unrotated solutions. Ten independent PCAs are performed, one for each monthly active area between September and June. The highest component (PC1) explains between 14% and 26% of hemispheric variance; the percentage of explained variance decreases rapidly after the first few components, with PC10 generally explaining less than 4%.

3.4.2. Stability of rotated solutions. For each month we examine the stability of solutions in which different numbers of components are retained for rotation. Potential solutions are identified by

examination of the scree plots. In addition, we include the 16-component solution for comparison. Stability is evaluated in three respects: the geographical patterns of coherent regions, the score time series, and regional–continental scale relationships. During most months several solutions give consistent results.

Choosing a 'best' solution is, therefore, subjective, and depends on the particular aspect of the solution that is of interest. Nevertheless, using the three criteria, we identify a best solution for each month, keeping in mind that the fifth section of this study is primarily focused on North American fluctuations. The suite of solutions examined, and our choice for best solution, are shown in Table I. Before going on to interpretation of PCA results (fourth section, part d), we discuss the sensitivity tests for 2 sample months, April and January, that exemplify the difficulties encountered in identifying a best solution. Scree plots for these months are shown in Figure 1.

3.4.3. Sensitivity tests for April. In accordance with the April scree plot, we examine solutions with 5, 10, 13, and 16 rotated components. In the PCA these groups of components explain 48.5%, 71.2%, 80.9%, and 88.6% of the variance, respectively, in Northern Hemisphere snow fluctuations (Table I).

The geographic patterns of coherent regions are generally stable between the different solutions (Figure 2). Over North America, two regions dominate the 16- and 13-component solutions, one over the northern Great Plains/southern Canadian Prairies, and one over the Canadian shield south of Hudson Bay. In the 10- and 5-component solutions these two regions are combined into one larger region, and in the 5-component solution this single region degenerates into two centres. Over Eurasia, the 16-, 13-, and 10-component solutions are consistent with the exception of one minor region in each solution. In the 5-component solution, two major regions are lost, and the shapes of two remaining regions tend to degenerate.

Score time series are consistent, especially in the 16-, 13-, and 10-component solutions. To indicate this, we show Pearson correlation coefficients between score time series from the 16-component solution and corresponding regions in the other solutions (Table II). Correlations tend to decrease as fewer components are retained, especially over North America when two regions are replaced by one region. However, even for the 10-component solution, values of $r \geq 0.9$ are still found.

We also examine the stability of regional–continental scale relationships in the different solutions. Cross-validated multiple linear regression results (Table I) show that the 16- and 13-component score time series explain the same portion of variance in the continental snow signals. In comparison to the 16- and 13-component solutions, the 10- and 5-component solutions explain more Eurasian variability but less North America variability.

A solution with fewer components, which is simpler, is preferable with all else being equal. The 16-component solution has no advantages over the 13-component solution; and the 5-component solution produces degenerated regional shapes. This leaves the 13- and 10-component solutions, of which the former is more advantageous for explaining North American variability, and the latter for explaining Eurasian variability. We choose the 13-component solution 'best' since North America is of particular interest for this study.

3.4.4. Sensitivity tests for January. January results are less stable in one regard: for the 8-component solution, the regional–continental scale relationship deteriorates over North America. The 13- and 11-component solutions are stable with regards to regional locations (except for small, minor regions) (Figure 3), correlation of the score time series (Table III), and continental multiple regressions (Table I). In the 8-component solution, however, PC4 in the northern US Great Plains weakens so that no grid cell has a loading factor ≥ 0.7, and that region therefore drops out of the solution. The removal of PC4 decreases the percentage of explained North American variance in the multiple regression by half compared to the 11-component solution; while over Eurasia the 8-component is consistent with the other solutions. For Eurasia the 8-component solution is simpler and just as effective, but for analysing North American snow extent the 11-component solution is best.

Table I. Summary of results from Northern Hemisphere Principal Components Analysis (PCA) and continental linear multiple regression analyses

	PCA results		Eurasia multiple regression results					North America multiple regression results				
	PCs	% var	*n*	*r*	*r*-CV	% var	Signif	*n*	*r*	*r*-CV	% var	Signif
September	16	90.3	6	0.79	0.47	22.1	0.012	3	0.59	0.32	10.2	0.07
	10	74.2	4	0.69	0.45	20.3	0.015	2	0.65	0.47	22.1	0.012
	8	**66.9**	**3**	**0.70**	**0.48**	**23.0**	**0.011**	**1**	**0.48**	**0.25**	**6.3**	**0.128**
	4	44.9	2	0.85	0.79	62.4	<0.01	1	0.46	0.22	4.8	0.156
October	16	89.1	5	0.91	0.79	62.4	<0.01	4	0.94	0.91	82.8	<0.01
	12	**77.6**	**2**	**0.89**	**0.79**	**62.4**	**<0.01**	**4**	**0.94**	**0.90**	**81.0**	**<0.01**
	9	66.9	3	0.90	0.82	67.2	<0.01	3	0.89	0.84	70.6	<0.01
	5	48.8	1	0.84	0.75	56.3	<0.01	2	0.89	0.87	75.7	<0.01
November	16	87.9	5	0.83	0.65	42.3	<0.01	5	0.91	0.85	72.3	<0.01
	12	**76.9**	**6**	**0.83**	**0.66**	**43.6**	**<0.01**	**4**	**0.91**	**0.85**	**72.3**	**<0.01**
	8	61.1	4	0.91	0.85	72.3	<0.01	3	0.89	0.86	74.0	<0.01
	6	51.4	3	0.85	0.79	62.4	<0.01	2	0.90	0.88	77.4	<0.01
December	16	88.2	7	0.91	0.73	53.3	<0.01	2	0.86	0.81	65.6	<0.01
	13	80.1	7	0.91	0.74	54.8	<0.01	2	0.85	0.80	64.0	<0.01
	10	70.0	5	0.91	0.80	64.0	<0.01	2	0.84	0.79	62.4	<0.01
	7	**57.7**	**5**	**0.89**	**0.76**	**57.8**	**<0.01**	**2**	**0.90**	**0.87**	**75.7**	**<0.01**
January	16	87.9	8	0.95	0.85	72.3	<0.01	3	0.79	0.62	38.4	<0.01
	13	79.3	6	0.91	0.81	65.6	<0.01	3	0.85	0.75	56.3	<0.01
	11	**72.8**	**5**	**0.88**	**0.77**	**59.3**	**<0.01**	**4**	**0.89**	**0.79**	**62.4**	**<0.01**
	8	61.0	3	0.87	0.81	65.6	<0.01	2	0.66	0.55	30.3	<0.01
	5	46.4	2	0.73	0.61	37.2	<0.01	1	0.48	0.33	10.9	0.122
February	16	88.6	7	0.86	0.69	47.6	<0.01	1	0.94	0.92	84.6	<0.01
	14	83.2	5	0.91	0.74	54.8	<0.01	2	0.96	0.95	90.3	<0.01
	10	70.1	5	0.90	0.80	64.0	<0.01	1	0.94	0.93	86.5	<0.01
	7	57.4	2	0.67	0.57	32.5	<0.01	1	0.95	0.95	90.3	<0.01
	4	**41.6**	**3**	**0.91**	**0.86**	**74.0**	**<0.01**	**1**	**0.96**	**0.96**	**92.2**	**<0.01**
March	16	87.1	6	0.94	0.86	74.0	<0.01	2	0.90	0.87	75.7	<0.01
	10	**69.0**	**3**	**0.90**	**0.86**	**74.0**	**<0.01**	**2**	**0.94**	**0.91**	**82.8**	**<0.01**
	6	52.2	3	0.89	0.83	68.9	<0.01	1	0.88	0.85	72.3	<0.01
April	16	88.6	7	0.90	0.79	62.4	<0.01	2	0.95	0.94	88.4	<0.01
	13	**80.9**	**5**	**0.88**	**0.79**	**62.4**	**<0.01**	**2**	**0.96**	**0.94**	**88.4**	**<0.01**
	10	71.2	5	0.93	0.86	74.0	<0.01	1	0.92	0.91	82.8	<0.01
	5	48.5	3	0.90	0.85	72.3	<0.01	1	0.89	0.87	75.7	<0.01
May	16	87.9	6	0.81	0.70	49.0	<0.01	3	0.82	0.72	51.8	<0.01
	8	**61.4**	**3**	**0.70**	**0.57**	**32.5**	**<0.01**	**2**	**0.85**	**0.80**	**64.0**	**<0.01**
	3	34.1	2	0.83	0.77	59.3	<0.01	1	0.79	0.74	54.8	<0.01
June	16	89.1	4	0.86	0.75	56.3	<0.01	3	0.73	0.61	37.2	<0.01
	7	61.3	2	0.78	0.72	51.8	<0.01	2	0.72	0.60	36.0	<0.01
	4	**46.6**	**3**	**0.92**	**0.89**	**79.2**	**<0.01**	**2**	**0.86**	**0.81**	**65.6**	**<0.01**

For each month, solutions retaining different numbers of components for rotation, as identified from scree plots, are shown. For PCA results the two columns are: the number components retained for rotation; and the cumulative % variance explained by all retained components. For each continental regression five values are shown: *n*, the number of components included in the regression (i.e. the number of coherent regions found on that continent); *r*, the Pearson correlation coefficient between observed and predicted continental signal; *r*-CV, correlation coefficient calculated from cross-validated predictions (see text for explanation);% var (r-CV^2), the percent variance explained by the cross-validated prediction; signif, the significance of *r*-CV (1-tailed, $n = 23$). Solutions in bold typeface are those chosen as most appropriate according to criteria discussed in text.

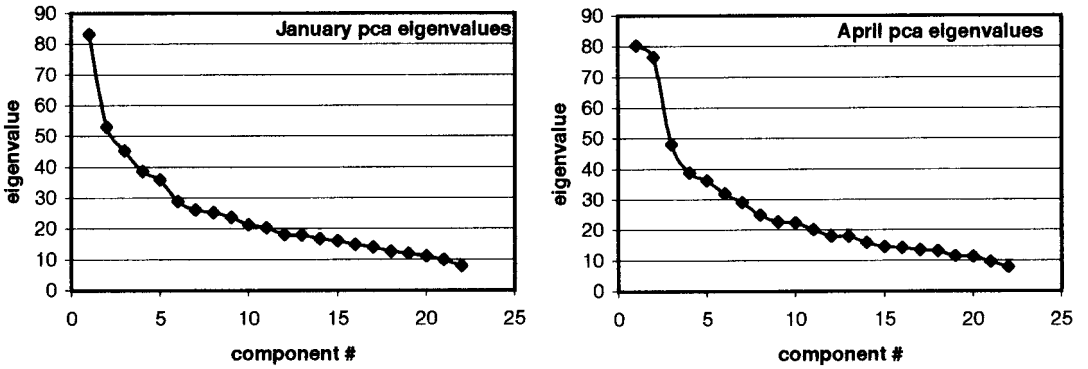

Figure 1. Scree plots for January and April. These plots show eigenvalue versus component number. 'Ends of shelves', which are used to determine potential subgroups of components to be retained for rotation, are identified by visual interpretation as described in text

4. RESULTS OF REGIONAL ANALYSIS

4.1. (a) Areas of active snow cover fluctuations

Areas of active snow cover fluctuations during each month (Figure 4) cover between 10% and 29% of the continental land area north of 20°N (Table IV). The largest active areas are found during October and November, when snow begins to accumulate over large portions of the continents. The smallest active areas are found at the ends of the season when the total snow covered area is small, and in mid-winter when interannual variability is minimal. In September and June the active areas are generally found north of 60°N, along with some mountain ranges farther south.

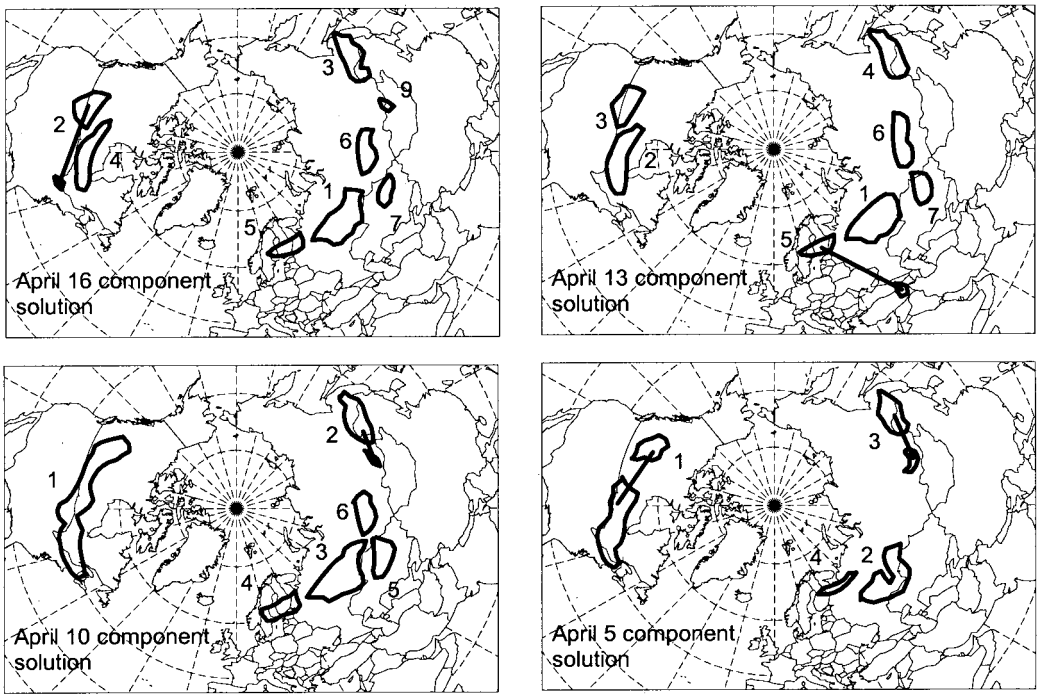

Figure 2. Regions of coherent snow fluctuations for different potential solutions for April. Each coherent region is indicated by the 0.7 component loading contour. Potential solutions chosen according to scree plot as discussed in text

Table II. Correlation coefficients between score time series from 16-component solution and score time series from corresponding regions in the April 13-, 10-, and 5-component solutions

	16-component PCs							
	PC1	PC2	PC3	PC4	PC5	PC6	PC7	PC9
13 components	0.99	0.99	0.97	0.96	0.98	0.97	0.91	na
10 components	0.98	0.80	0.91	na	0.96	0.89	0.77	na
5 components	0.88	0.67	0.82	na	0.72	na	na	na

All values are significant (2-tailed, $p = 0.01$, $n = 23$).
na = not available.

From December through March the active areas are located almost exclusively south of 47°N, because the land area north of that latitude is close to 100% snow covered. Two areas are exceptional in this regard. The high North American prairies remain active in winter because the dry climate and downsloping Chinook winds in the lee of the Rocky Mountains prevent perpetual snow cover. Also, portions of northern Europe remain active due to the influence of maritime air masses that maintain average winter surface temperatures above the latitudinal mean. The southernmost fringe of the active areas during winter months (about 30°N) includes a large swath of the Tibetan Plateau between around 80°E and 105°E longitude.

Active areas derived in this study are similar to the snow transient regions (STRs) of Groisman *et al.* (1994b) and the temperature sensitive regions (TSRs) of Karl *et al.* (1993) and Groisman *et al.* (1994b). STRs, like active areas, were defined according to snow cover variability, but on a seasonal time scale. During spring and fall, active areas indicate that the northern and southern portions of seasonal STRs are largely independent of each other on monthly time scales. TSRs, defined as areas where snow cover

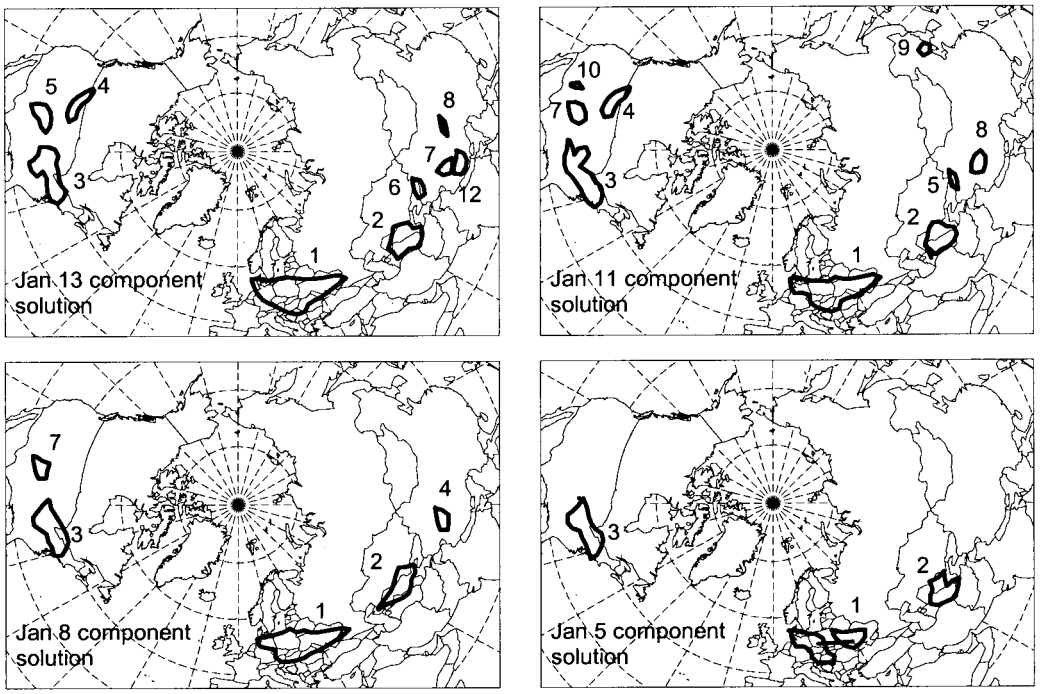

Figure 3. Regions of coherent snow fluctuations for different potential solutions for January. Each coherent region is indicated by the 0.7 component loading contour. Potential solutions chosen according to scree plot as discussed in text

Table III. Correlation coefficients between score time series from 16-component solution and score time series from corresponding regions in the January 13-, 11-, 8-, and 5-component solutions

	16-component solution									
	PC1	PC2	PC3	PC4	PC5	PC6	PC7	PC8	PC9	PC10
13 components	0.99	0.93	0.97	0.89	0.88	0.95	0.35	na	na	0.99
11 components	0.97	0.93	0.95	0.86	0.88	0.93	na	na	na	na
8 components	0.95	0.92	0.89	na	na	0.83	na	na	na	na
5 components	0.86	0.90	0.90	na	na	na	na	na	na	na

All values are significant (2-tailed, $p = 0.01$, $n = 23$).
na = not available.

frequency changes substantially between warm and cold years, are similar to STRs. This is not surprising considering the relationship between snow cover and air temperature.

4.2. (b) PCA: interpretation of results

Figure 4 shows the 0.7 loading contours of those components that are associated with coherent geographic regions for the 'best' solutions. Strong regional signals are prevalent over the Northern Hemisphere during all months. For each month, between one and four regions in North America, and two and six regions in Eurasia, are identified. In most months the four strongest PCs, plus up to six additional PCs, are retained for further analysis. Only in November and January are any components higher than PC7 associated with coherent regions.

4.2.1. Spatial characteristics of regions. Coherent regions cumulatively cover between 11% and 27% of the monthly active areas, and thus 2–6% of the Northern Hemisphere land area north of 20°N (Table IV). The median areal extent of coherent regions is approximately 0.4×10^6 km^2. Higher order PCs by definition explain more variance than lower order PCs; in addition, they tend to cover larger areas. Median areas for PC1 and PC2 are between $\cong 0.7$ and $\cong 1 \times 10^6$ km^2, while PC5 and PC6 median areas are less than $\cong 0.4 \times 10^6$ km^2. The largest region of any month (PC1 of October), which covers approximately 1.9×10^6 km^2, includes most of north-eastern Russia, extending from Finland (30°E) to the Mongolian Plateau (100°E) (Figure 4), and explains 13% of the hemispheric variance.

There is only one example of a single signal being associated with two distinct, nonadjacent regions: April PC5, for which we find 0.7 loading contours over Scandinavia and also over the mountains of eastern Turkey (Figure 4). During other months some signals do have more than one 0.7 loading contour; however, in those cases the region between the contour lines is either not part of the active area, or not dominated by any other signal.

4.2.2. Temporal characteristics of snow anomalies. We examine regional time series from six longitudinal sectors across the Northern Hemisphere: western North America (west of 90°W); eastern North America (east of 90°W); Europe (west of 40°E); western Asia (40°E–70°E); central Asia (70°E–100°E); and eastern Asia (east of 100°E). (These are partially subjective boundaries based on the locations of coherent regions.) We find two interesting features, both of which occur during winter and spring, associated with the following: the month-to-month persistence of snow anomalies; and a step-change in snow extent around the mid-1980s. Figure 5 shows selected time series.

The month-to-month persistence of regional snow anomalies is quantified using Pearson correlation coefficients between PC score time series from consecutive months (Table V). Over western North America and Europe we find significant persistence from January–February through March–April. This conclusion remains true for the pre- and post-1987 periods independently, when a step-change in mean snow extent is identified (see discussion below). Over eastern North America and Asia we find no sectors with 2 consecutive months of significant correlations. This corroborates the results of Walsh *et al*. (1982),

who examined persistence of snow anomalies over North America and found that the western and midwest US have greater 1- and 2-month persistence than the eastern US.

Anomalously high or low snow extent is not usually maintained throughout the entire snow season, even over western North America and Europe where significant persistence is found. However, several seasons were exceptional in that respect. For example, over western North America, high (low) snow cover extent persisted for most of the 1978–1979 (1980–1981) snow season. Over Europe the 1979–1980 season had numerous above-average months, and the 1974–1975 and the 1989–1990 seasons had several below-average months. Over eastern North America, the 1977–1978 and 1978–1979 snow seasons had high coverage during several months, while the 1982–1983 season generally had below-average snow extent. Other seasons of note in this regard include: 1973–1974 and 1974–1975 over western Asia; 1982–1983 over central Asia; 1975–1976 and 1980–1981 over eastern Asia.

Regional time series (Figure 5) also indicate that a change in mean of snow extent over several regions occurred around 1987. This is most obvious over several Eurasian sectors, but it is also true over North

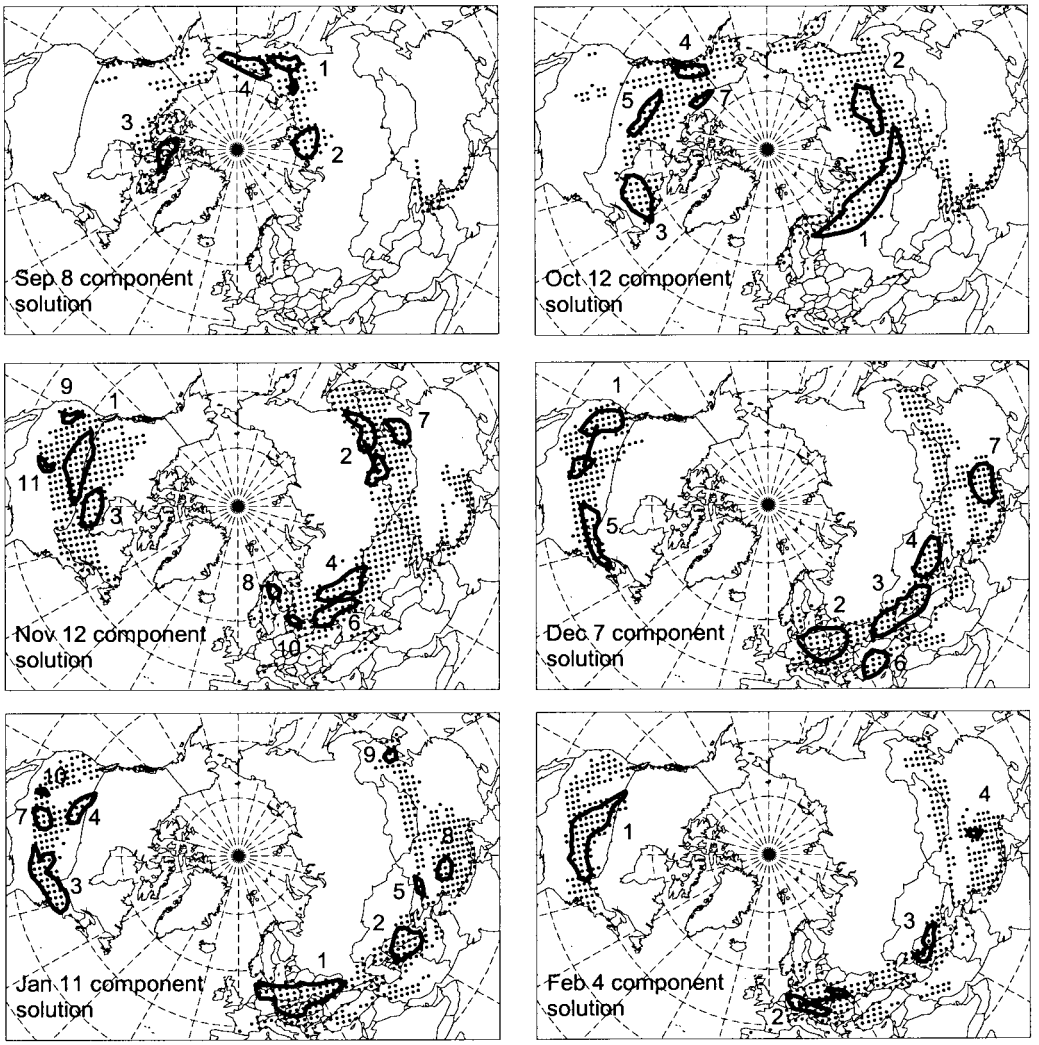

Figure 4. Areas of 'active' snow extent fluctuations, and regions of 'coherent' snow fluctuations, for September through June. Grid cells included in the active areas for each month are shown as black dots. Each coherent region is indicated by the 0.7 component loading contour from the 'best' solution for each month. PC numbers are shown next to corresponding regions. See text for definitions of 'active' regions and 'best' solutions

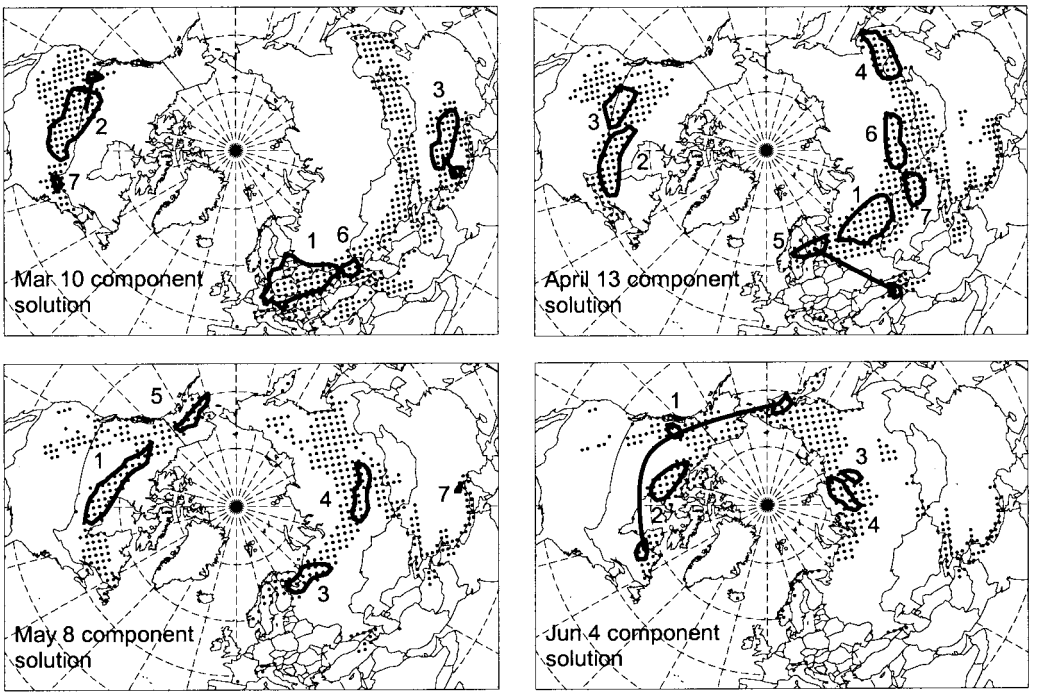

Figure 4 (*Continued*)

America. The European signal is strongest. Between 1988 and 1994 only a few PC score values are positive, while many are below -1 S.D.; particularly low values are found in 1989 and 1990. Over central Asia the late 1980s were low from February through April. Over eastern Asia the only coherent region identified was in April, when only one PC score value since 1985 is above-average. Over eastern North America between 1987 and 1991 no PC score values are greater than $\cong 0.5$. Over western North America

Table IV. Geographic extent of active areas and coherent regions for each month

	Active area (10^6 km^2)	Number of regions	Total regional area (10^6 km^2)	Active/NH (%)	Regional/NH (%)	Regional/ active (%)
September	8.5	4	1.6	10.6	2.0	18.7
October	21.0	6	4.2	26.3	5.3	20.2
November	22.6	10	4.3	28.3	5.4	19.0
December	17.8	7	3.5	22.3	4.4	19.8
January	15.4	9	4.1	19.3	5.1	26.5
February	14.6	4	2.1	18.3	2.7	14.5
March	17.2	5	3.2	21.5	4.0	18.7
April	18.1	7	4.5	22.7	5.7	25.0
May	15.9	5	2.6	20.0	3.3	16.3
June	13.5	4	1.6	16.9	2.0	11.8
Mean	16.5	6.1	3.2	20.6	4.0	19.1
Median	16.5	5.5	3.4	20.7	4.2	18.9
Max	22.6	10	4.5	28.3	5.7	26.5
Min	8.5	4	1.6	10.6	2.0	11.8

Columns, from left to right, are: month; active area; number of regions; sum of regional areas; active area expressed as percentage of total Northern Hemisphere land area north of 20°N; sum of regional areas expressed as percentage of total Northern Hemisphere land area north of 20°N; sum of regional areas expressed as percentage of active area. Total Northern Hemisphere land area north of 20°N is approximately 79.8 million km^2.

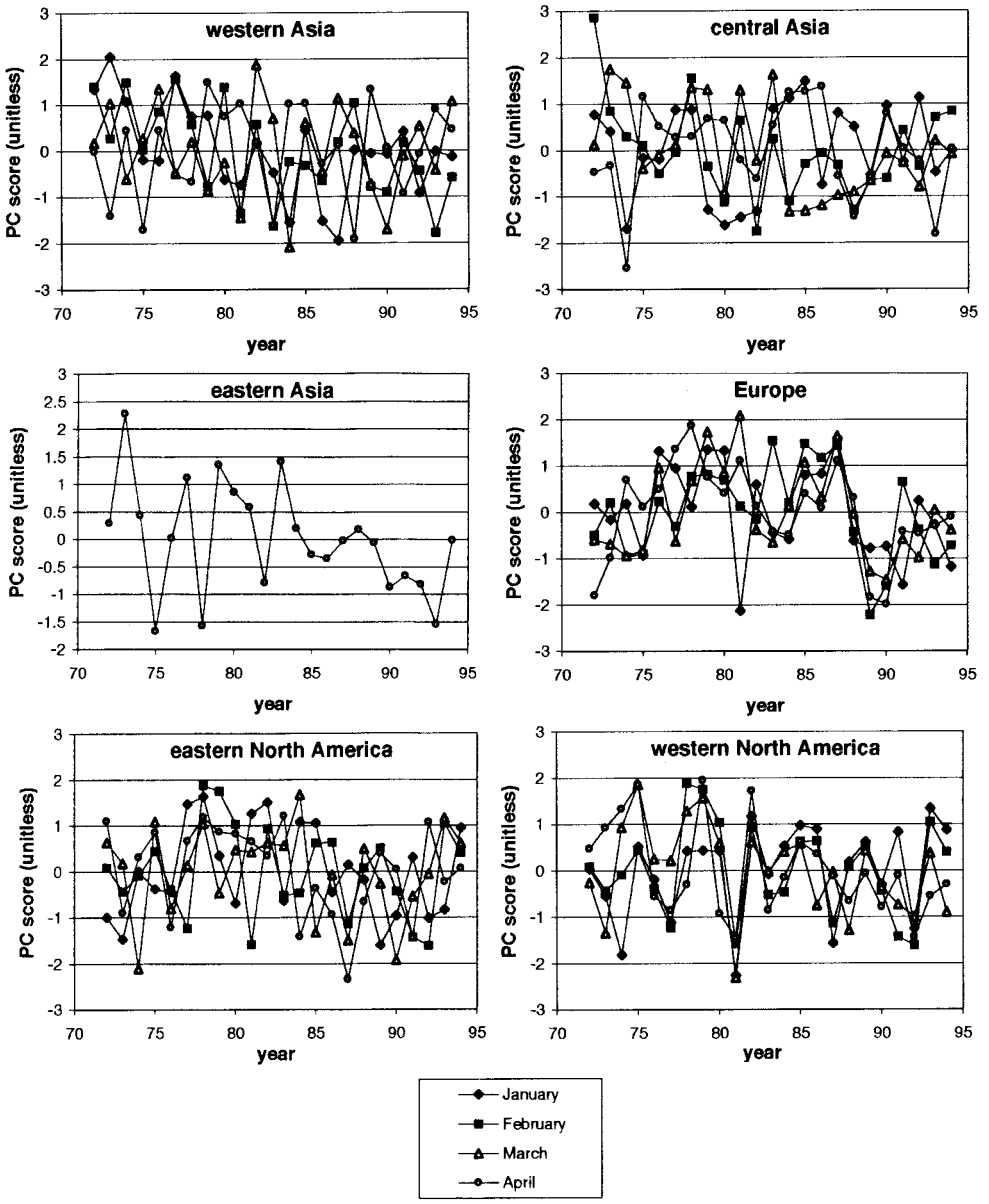

Figure 5. Score time series for selected regions and months

between 1987 and 1992 we find relatively few values > 0.5 S.D., no values > 1, and several years with negative anomalies below -1. These low regional values deduced from the PCA are reflected in hemispheric scale snow extent as calculated directly from the NOAA observations. Between 1988 and 1995 annual average Northern Hemisphere snow cover extent was 24.2×10^6 km^2, compared to the 1972–1985 average of 25×10^6 km^2 (Robinson and Frei, 1997). Through January 1999, annual and spring snow extent across the hemisphere have remained at these lower levels (Robinson, 1999). Spring snow extent is especially important climatologically due to the pronounced effect of snow cover on temperatures during that season (Groisman *et al.*, 1994a).

Table V. Monthly persistence in snow covered area over Northern Hemisphere longitudinally defined sectors

	October–November	November–December	December–January	January–February	February–March	March–April	April–May
W. N.A.	−0.20	0.14	0.03	0.66**	0.62**	0.56**	0.19
E. N.A.	na	na	0.09	0.07	0.23	0.27	na
Europe	na	0.28	−0.40	0.42*	0.63**	0.65**	na
W. Asia	0.38	0.23	0.55**	0.40	0.25	−0.37	0.31
C. Asia	na	na	0.11	0.17	0.49*	−0.29	0.38
E. Asia	0.35	na	na	na	na	na	na

Areas are defined as: western North America (west of 90°W); eastern North America (east of 90°W); Europe (west of 40°E); western Asia (40°E–70°E); central Asia (70°E–100°E); and eastern Asia (east of 100°E). Values are Pearson correlation coefficients between primary PC score time series in each sector.
* $p<0.05$; ** $p<0.01$ (1-tailed, $n=23$). January through April score time series are shown in Figure 5.

4.3. (d) Regional–continental scale interactions

The PCA results described above reveal the portion of the variance in snow extent across the *hemisphere* explained by each PC; in this section, interactions between the regional and *continental* scales are examined. Hemispheric scale forcing explains only part of the continental scale variability of snow extent. A simple linear correlation between North American and Eurasian continental snow extent (Table VI) shows that, although there is significant intercontinental correlation, the percent variance explained is generally less than 50%, corroborating the results of earlier reports (Iwasaki, 1991; Gutzler and Rosen, 1992; Robinson *et al*., 1995). This is also corroborated by the regional analysis presented here, which shows that intercontinental correlations in regional snow signals are insignificant. These results indicate that physical mechanisms associated with the deposition and maintenance of snow operate at several spatial scales.

Mean Eurasian snow extent, as well as interannual variability, are generally twice the magnitude of North American snow extent. Mean monthly snow extent across North America peaks at approximately 15×10^6 km^2 in January and February; over the Eurasian land mass, which is far more expansive, peak snow extent is almost twice as large. Similarly, the range and S.D. of monthly-averaged snow extent across Eurasia is generally twice as large as over North America, leading to Coefficient of Variation (COV) values that are comparable. The largest COVs occur at the end of the snow season.

Results of multiple linear regression analyses between continental snow extent (the dependent variable) and regional time series (the independent variables) indicate that much of the variance in continent-wide snow extent can be explained by regional signals (Table I). In all months except September the observed and predicted continental time series are positively and significantly correlated (cross-validated correlation, $p=0.01$, df $=21$, 1-tailed). Between October and June, regional variations explain $>60\%$ of the variance of North American snow extent fluctuations in all months (maximum $=92.2\%$ in February). Over Eurasia, $>60\%$ of the variance is explained by regional signals during October, February, March, April, and June; only in September and May is $<40\%$ of the variance explained. This relationship is important for reconstructing pre-satellite era snow extent from limited historical station observations (see Frei *et al*., 1999).

Table VI. Pearson correlation coefficients between North American and Eurasian snow extent, 1972–1994

January	February	March	April	May	June	July	August	September	October	November	December
0.48*	0.35	0.22	0.03	0.62*	0.82*	0.75*	0.67*	0.71*	0.46*	0.47*	0.68*

* $p\geq 95\%$ ($n=23$, 2-tailed). No serial autocorrelation in either time series was found.

5. METHODOLOGY FOR CIRCULATION ANALYSIS OVER NORTH AMERICA

Composite analysis is used to examine circulation and teleconnection patterns, cyclonic activity, regional temperatures, snowfall, and precipitation fluctuations associated with snow extent over North American coherent regions. The temporal domain includes the 22 years from 1972 through 1993, the period of overlap between the remotely-sensed and station-based data sets. The spatial domain includes the North American sector between 30°N and 80°N latitude, and between 20°W and 180°W longitude. This area extends far enough west and east to identify relationships between snow extent and circulation patterns over the eastern Pacific and western Atlantic Oceans. A similar analysis of Eurasian snow extent is planned, pending completion of a quality control of station observations recently made available from the former Soviet Union and China.

In the first step, snow extent in each region is ranked, and composites are made of the 500-mb geopotential height fields for the 5 years in the upper quartile (highest snow extent) and the 5 years in the lower quartile (lowest snow extent). Regionally-averaged snowfall, total precipitation, and surface maximum and minimum temperatures are also composited for high and for low years using observations from meteorological stations that are located within coherent regions.

Composite 500-mb height fields are calculated by averaging the fields from each of the 5 high, and the 5 low, snow extent months. Composite differences are calculated by subtracting the 'low' from the 'high' 500-mb fields. The statistical significance of composite 500-mb height differences at each grid point is assessed using the two-tailed Student's t-test, with differences significant at $\geq 95\%$ indicated on the composite difference maps. This method, by which significance at each grid point is assessed individually, does not test for field significance. Due to the limited number of years in each composite, we rely on our evaluation of the physical plausibility of the results, and examination of Daily Weather Maps and other surface observations, rather than more detailed procedures (e.g., Livezey and Chen, 1983), to address the issue of field significance. Sample composite maps of the 500-mb height fields for November through March are shown in Figures 6–9.

To analyse cyclonic activity, the number of surface cyclones associated with high and with low snow extent are tabulated for the entire North American sector, as well as for critical sub-areas (Table VII). These sub-areas are defined according to the composite difference 500-mb charts. For western coherent regions, cyclonic activity is tabulated within four sub-areas: Iceland, the Aleutians, central North America, and Hudson Bay/central Canada. For eastern coherent regions, the sub-areas are: the northern North Atlantic sector, the southern North Atlantic sector, and the Aleutians. These sub-areas cover most of the North American sector, including the locations of most frequent cyclogenesis north of 30°N: Alberta, the Great Basin, Colorado, the East Coast, and the Northwest Territories (Whittaker and Horn, 1981).

6. RESULTS OF CIRCULATION ANALYSIS OVER NORTH AMERICA

6.1. (a) Western regions

In a typical November, the troposphere is in adjustment, switching into a more winter-like pattern with the monthly average Rossby wavelength increasing, the eastern trough deepening, and North American circulation becoming more meridional (Harman, 1991). Much of North America receives its first snowfall of the season during that month. Over western North America, high snow extent during November is associated with a displacement of the North American ridge 20–30° westward from its climatologically mean position, producing meridional circulation with a strong jet, northerly flow over the west, and 'troughing' in the east (Figure 6a). Snowfall typically results from migrating shortwave disturbances. During low snow years, tropospheric circulation is late in assuming its typical winter mode: the polar jet, and polar air masses, remain over central and northern Canada; 'troughing' persists over the Gulf of Alaska; and weak, zonal, or split flow dominates over the continent (Figure 6b). The 500-mb height

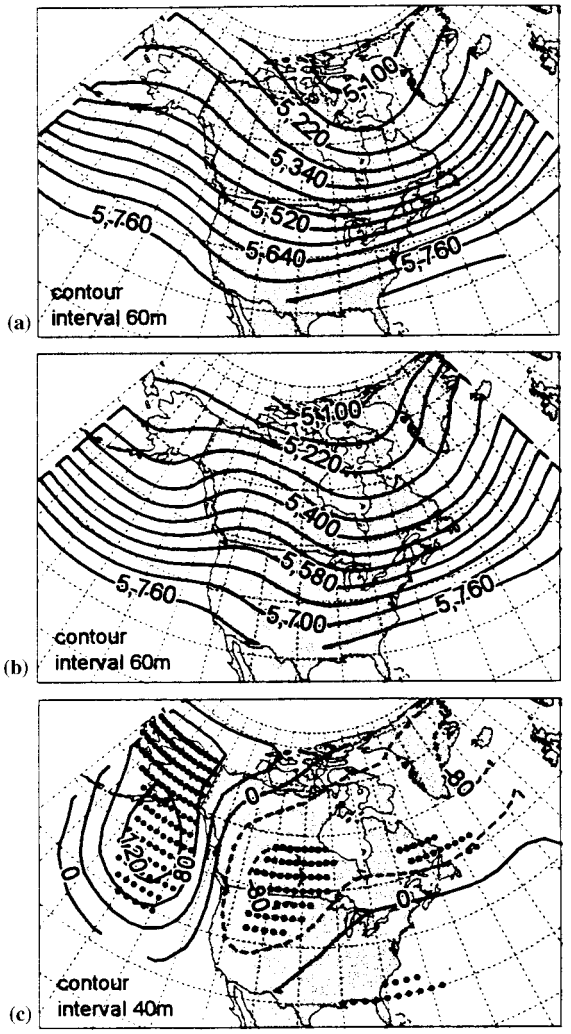

Figure 6. Composite 500-mb geopotential heights for November PC1. (a) (top) composite for years of high snow extent; (b) (middle) composite for years of low snow extent; (c) (bottom) composite difference (a)–(b). In (c), negative contours are dashed, and grid cells with difference significant at 95% according to the Student's *t*-test are indicated with black dots. See Figure 1 for region location

difference field (Figure 6c) indicates two 'centres of action' for mid-tropospheric circulation: one directly over the region, where below-average 500-mb heights prevail during extensive snow years; and the second over the eastern Pacific Ocean/Gulf of Alaska, with above-average heights. These circulation differences are reflected in the storm track statistics. During years with less extensive snow, the southwesterly flow over the west coast helps to steer cyclonic systems towards the north. During extensive snow years, the westward-shifted ridge helps to steer cyclones further southward over the western US. During November, snow extent is determined by both the deposition of snow and the advection of cold air masses required to maintain the snow pack.

When snow is already on the ground at the beginning of the month, the southward advancement of polar air masses that maintain below-freezing temperatures becomes increasingly important, while the frequency of migrating shortwave disturbances, or other snowfall-producing mechanisms, becomes less important for determining snow extent. For example, in December 500-mb centers of action are found in similar positions to centres of action in November, with extensive snow cover occurring when the mean western ridge is shifted westward over the eastern Pacific. However, the relationships between snow extent

and both cyclonic activity and snowfall weaken, while the correlation between snow extent and temperature is higher in December than in November (Table VIII).

During March, the atmosphere is typically in transition between winter and spring, with the ridge/trough system migrating westward, and troughs becoming more frequent over the central continent (Harman, 1991). The area encompassed by PC2, located over central North America, still receives a significant portion of its annual snowfall during March (Harrington *et al*., 1987). In years with extensive March snow extent over this region, westward migration of the mean trough occurs earlier and below-average 500-mb heights are found directly above. During low snow years, the central continent experiences more frequent ridging; troughs are more frequent over the Aleutians (Figure 7), and the frequencies of storm tracks are increased over Alaska and northern Canada. During March, the eastern Pacific centre of action is weaker than during earlier months (compare Figure 7c with 6c).

6.2. (b) Eastern regions

During winter (December, January, February (D, J, F)), snow extent over eastern North America is associated with circulation wave patterns over the eastern continent and the western Atlantic Ocean.

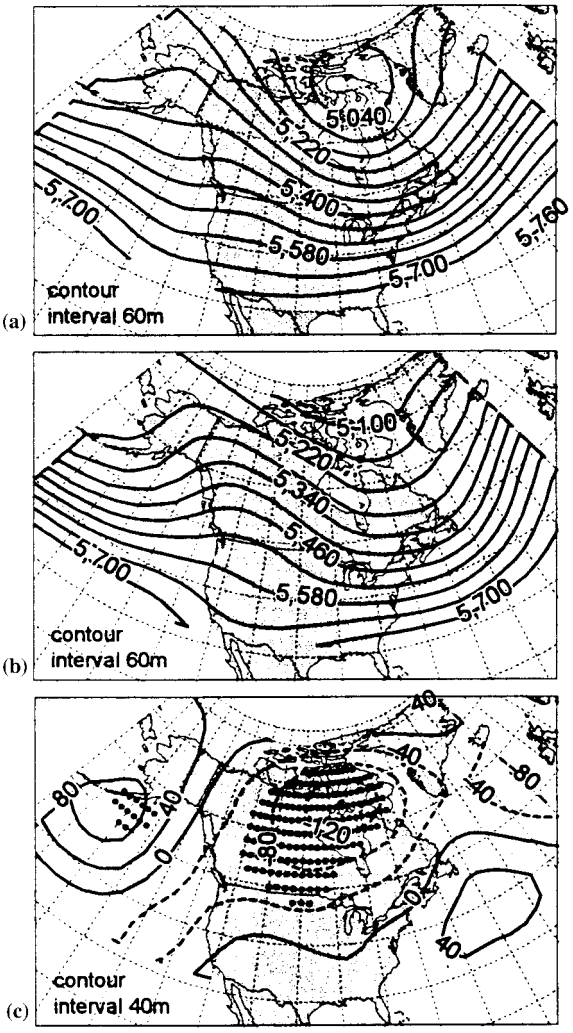

Figure 7. Same as Figure 6 except for March PC2

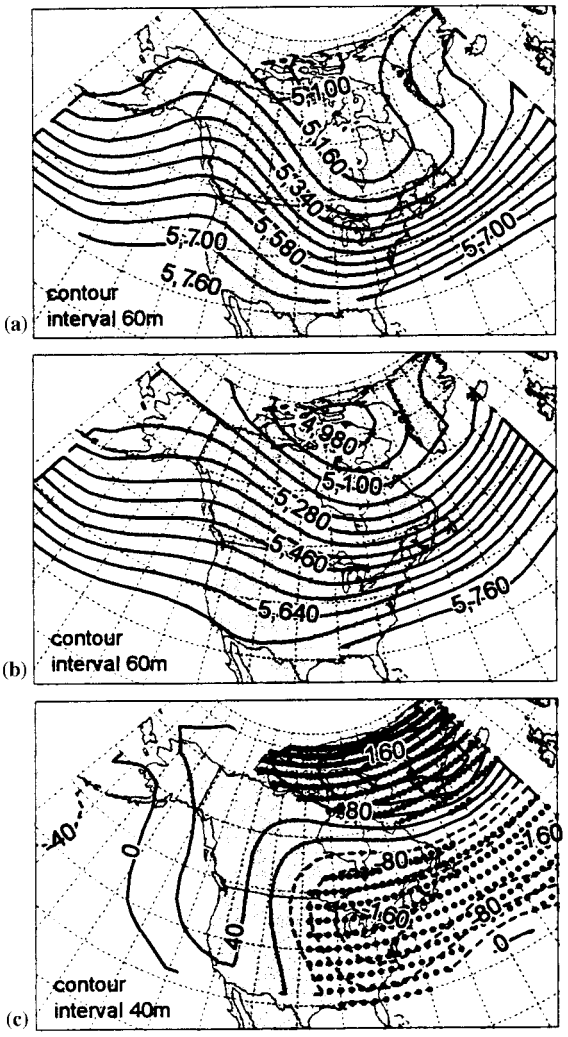

Figure 8. Same as Figure 6 except for December PC5

During high snow years, a high amplitude wave and meridional flow dominate over the continent, producing extensive snowfall in the east (e.g., Figure 8a). The strongest height gradients along the east coast are concentrated between 35°N and 45°N, preferentially steering surface cyclones over the mid-latitude, rather than high-latitude, North Atlantic Ocean. These conditions are associated with above-average snowfall and below-average temperatures in this region (Table VIII). In contrast, during months of low snow extent, temperatures are above-average and snowfall is below-average (Table VIII); 500-mb height gradients are weaker (Figure 8b); and, no preferential steering of cyclones between the mid-latitude and northern North Atlantic is observed. Composite difference 500-mb charts (Figure 8c) indicate two centres of action, representing a north–south dipole. One is over the northern North Atlantic (near southern Greenland) north of 55°N, where high snow extent is associated with above-average 500-mb heights (i.e., a weakened Icelandic Low). The second centre of action is found south of 55°N, and is less confined longitudinally, covering eastern North America and the western Atlantic. During years with extensive snow over the east, the southern centre of action has below-average 500-mb heights, representing a weakening of the climatologically mean ridge in that area, and a more southerly storm track. (These results are discussed in relation to the North Atlantic Oscillation in part d of this section.)

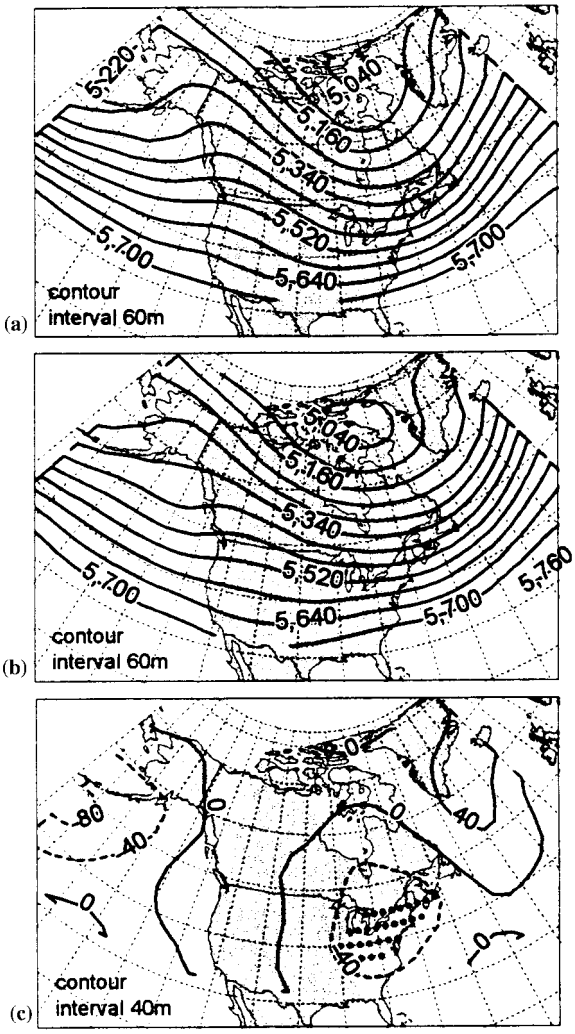

Figure 9. Same as Figure 6 except for March PC7

These relationships (Figure 8) reflect the predominance of daily synoptic patterns associated with snowfall and low temperatures. A number of tropospheric patterns interact to produce conditions necessary for large snowfall events along the east coast (Kocin and Uccellini, 1990). At the surface, ridging dominates over the Canadian maritime provinces, ushering cold air southward. Cold air damming

Table VII. Critical areas for tabulation of cyclonic activity associated with regional snow extent

Region	Latitude range	Longitude range
North America	30°N–80°N	20°W–180°W
Iceland	50°N–80°N	20°W–70°W
Aleutian	40°N–70°N	130°W–180°W
Central N.A.	30°N–55°N	90°W–120°W
Hudson Bay	55°N–80°N	80°W–120°W
Northern N. Atlantic	55°N–80°N	20°W–90°W
Southern N. Atlantic	30°N–55°N	20°W–90°W

Table VIII. Pearson (Spearman) correlation coefficients between PC score time series and snowfall, maximum temperature, minimum temperature, and total precipitation for each region (1972–1993)

Region	Snowfall	Max. temp.	Min. temp.	Precipitation
November PC1	0.83** (0.83**)	−0.67** (−0.75**)	−0.57** (−0.65**)	0.76** (0.70**)
December PC1	0.76** (0.77**)	−0.87** (−0.85**)	−0.73** (−0.66**)	0.10 (0.15)
December PC5	0.79** (0.75**)	−0.77** (−0.73**)	−0.64** (−0.59**)	−0.19 (−0.15)
January PC3	0.79** (0.84**)	−0.83** (−0.79**)	−0.82** (−0.72**)	0.14 (0.11)
January PC4	0.43* (0.45*)	−0.50* (−0.37)	−0.41** (−0.27)	0.51* (0.53*)
February PC1	0.75** (0.79**)	−0.91** (−0.91**)	−0.88** (−0.83**)	0.20 (0.21)
March PC2	0.74** (0.67**)	−0.84** (−0.86**)	−0.67** (−0.69**)	0.02 (−0.03)
March PC7	0.65** (0.61**)	−0.72** (−0.69**)	−0.63** (−0.64**)	−0.06 (−0.03)

* $p \geq 95\%$; ** $p \geq 99\%$ ($n = 22$, 2-tailed).

east of the Appalachians increases baroclinicity along the continental margin, and contributes to the steering of storms northward along the east coast (nor'easters). The eastern 500-mb trough is typically deepened, has its centre located 5–10° south of its usual position over Hudson Bay, and has negative tilt with diffluent flow east of the trough axis. Meridional flow, with increased amplitude and decreased wavelength, dominates over the continent, increasing the advection of absolute vorticity. Occasionally, this pattern is accompanied by a secondary low associated with Colorado Lows that bring maritime tropical air north-eastward across the continent, and causing frontal precipitation. For example, in January and February, a region of significant snowfall is found in a southwest to northeast band stretching from the southern plains to the northeast (Harrington *et al.*, 1987).

Other 500-mb patterns are associated more with the maintenance of low temperatures than with snowfall. The eastern trough centre can be situated as far east as Newfoundland, a displacement of 20–30° longitude from its usual position. Such a pattern ushers polar or Arctic air masses southward, blanketing the north-eastern US with frigid air and preventing snow melt. Blocking over Greenland is also associated with the southward displacement of cold air masses, but was found by Kocin and Uccellini (1990) to occur during only about half of all large eastern snow storms.

During periods of ablation, snow extent becomes disassociated from tropospheric dynamics. For example, in March, the southern boundary of the snow line over the eastern US recedes northward. This can be observed in Figure 4, where the areas of active snow fluctuations for March and April hardly overlap. The magnitudes of 500-mb composite height differences between high and low snow extent for March PC7 (Figure 9c) are small compared to earlier months, and are statistically significant only directly over the region. Although there is little difference in cyclonic activity between high and low snow cover months, snow extent remains significantly correlated to snowfall and temperature (Table VIII). Over this region, snow extent is poorly linked to synoptic conditions.

Other reports have shown that during spring, strong associations between snow extent and temperature are maintained, while the effects of mid-tropospheric dynamics appear to be diminished. Over open sites such as the North American plains, the solar zenith angle decreases during spring, radiative fluxes become a larger percentage of the surface energy budget, and the local thermal effect of snow cover increases. The increased importance of regional radiational forcing, and the enhanced temperature-albedo feedback effect of the snow cover itself, play a role in linking temperatures to snow extent (Dewey, 1977; Walsh *et al.*, 1982; Baker *et al.*, 1992). Over the forested north-eastern US, both sensible and latent energy fluxes contribute to enhanced depressions of daytime maxima over snow covered lands during transition seasons (Leathers *et al.*, 1995). On the hemispheric scale, Groisman *et al.* (1994a) found that snow cover exerts its largest effect on temperatures during spring, despite the fact that the area covered by snow is much greater during January and February. Ross and Walsh (1986) identified strong associations between continental snow cover and circulation conditions during the mid-winter months, but failed to find such a relationship during March. Thus, on regional to continental scales, the control of dynamics over snow extent is diminished during the ablation season as snow cover plays a larger role in determining the regional thermal environment.

6.3. (c) Pacific teleconnections and snow extent over western North America

The 500-mb height composite difference charts (e.g., Figure 6c) indicate two strong centres of action, with monthly dependent locations, associated with western snow extent. One node is found over the eastern North Pacific, and one is over western North America. We define the Western North American Snow Index based on the monthly values of these nodes:

$$\text{Western N.A. Snow Index} = z^*(\text{western North America}) - z^*(\text{North Pacific})$$

where z^* is the standardized 500-mb height taken at the node centres. Defined in this way, positive values of the index represent more meridional circulation, with stronger ridging over the western US; negative values indicate more zonal flow.

Correlations between this index and western snow extent are significant and positive for all months (Table IX, first column). This index is also significantly correlated ($p = 0.01$, $n = 23$, 2-tailed) to North American continental scale snow extent during November ($r = 0.56$) and December ($r = 0.57$), as most snow accumulation over North America during those months occurs over the western part of the continent.

These node locations are similar to those typically associated with the PNA teleconnection index. This indicates that the PNA may be related to snow extent over this region, as indicated by Gutzler and Rosen (1992) and Brown and Goodison (1996). Here, we compare these results to more traditional definitions of the PNA index involving three nodes. Wallace and Gutzler (1981) and Leathers *et al.* (1991) defined centres of action on the seasonal time scale. Barnston and Livezey (1987) defined centres of action on the monthly time scale. We define third nodes from this analysis based on weak centres of action observed over the south-eastern US. The traditional PNA index is defined as:

$$\text{PNA Index} = -z^*(\text{North Pacific}) + z^*(\text{western North America}) - z^*(\text{Gulf Coast})$$

where z^* is the standardized 500-mb height taken at the node centres. In some studies a fourth node, found in the subtropical Pacific Ocean, is identified. This node is omitted here as it is not required for the index to capture fluctuations in the wave energy propagating over the temperate land area (Leathers *et al.*, 1991).

Western snow extent is significantly correlated to the PNA index during November and December, regardless of which definition of node location is used. During other months, the correlation is not robust with regard to the choice of centres of action (Table IX). Gutzler and Rosen (1992) found significant correlations during December (-0.64) and January (-0.54) which are in close agreement with results from this analysis; but during February, they found no significant correlation. The circulation analysis presented here suggests an explanation for these results: North America snow extent during February is associated with oscillations over the Atlantic Ocean, rather than the Pacific. However, Leathers *et al.* (1991) found that the PNA index *is* related to temperature and precipitation over the continent during

Table IX. Pearson correlation coefficients between western snow extent and teleconnection indices defined by several authors

	Snow Index (Two nodes)	Snow Index (Three nodes)	Barnston and Livezey	Leathers *et al.*	Wallace and Gutzler
November	0.82**	−0.67**	−0.51*	−0.56**	−0.53*
December	0.47*	−0.65**	−0.60**	−0.52*	−0.46*
January	0.62**	−0.5*	−0.27	−0.38	−0.35
February	NA	NA	−0.17	−0.28	−0.20
March	0.50*	−0.49*	0.01	−0.25	−0.22

For November, Barnston and Livezey (1987) defined the West Pacific Oscillation instead of the PNA. The third node from this analysis is taken from weak centres of action found over south-eastern US.
* $p \geq 95\%$, ** $p \geq 99\%$ (2-tailed, $n = 23$). NA: not applicable.

Table X. Pearson correlation coefficients between eastern snow extent and teleconnection indices defined by several authors

	December PC5	January PC3	February PC1	March PC7
Snow Index	0.68**	0.71**	0.51*	na
NAO-B&L	0.55**	0.36	0.50*	−0.02
WAO-W&G	−0.34	0.49*	0.09	−0.03

* $p \geq 95\%$; ** $p \geq 99\%$ (2-tailed, $n = 23$).
'na' means that no snow index was defined for March in this analysis.

winter and early spring: they attribute this to the dominance of synoptic scale controls on precipitation during those seasons.

These somewhat contradictory results can be explained by examination of the 500-mb height fields during high and low snow months in the west (Figure 6). Synoptic control of western snow extent depends mostly on the location of the ridge axis, not on the wave amplitude. High snow extent is generally associated with an expansion of the eastern trough over the western land area, and a westward shift by 20–30° longitude of the western ridge/Aleutian trough system. In contrast, during periods of low snow extent, the ridge is found closer to its climatologically mean position over western North America. The PNA index, on the other hand, is a good measure of the wave amplitude, but is only secondarily affected by changes in the position of the mean wave pattern (Leathers and Palecki, 1992). Thus, one would expect some relationship, albeit a weak one, between the PNA and snow extent.

The two-node Western N.A. Snow Index is superior to the standard three-node indices for explaining variations in snow extent over western North America. The two-node index captures the shift in ridge location, which is more important than wave amplitude, for determining western snow extent.

6.4. (d) Atlantic teleconnections and snow extent over eastern North America

500-mb height composite difference charts (e.g., Figure 8c) indicate that during winter (D, J, F) a meridional dipolar teleconnection pattern influences snow extent over eastern North America. The northern node is centred over southern Greenland, and the southern node is found over the mid-latitude North Atlantic. The Eastern North American Snow Index, which is based on these nodes, is defined below.

$$\text{Eastern N.A. Snow Index} = z^*(\text{northern North Atlantic}) - z^*(\text{mid-latitude North Atlantic})$$

where z^* is the standardized 500-mb height taken at the monthly node centres. High values indicate a weakened Icelandic Low associated with a more southerly storm track. Significant correlations between the Eastern North American Snow Index and snow extent are found during December, January, and February (Table X). During February, when one regional signal dominates the entire continent, the Snow Index is also significantly correlated to snow extent over the entire North American continent ($p = 0.05$, $n = 23$, 2-tailed).

The teleconnection pattern identified here resembles known teleconnection patterns over the North Atlantic Ocean. However, the Snow Index is a better indicator of snow extent than indices derived strictly from circulation observations. The locations of our northern nodes are close to the Barnston and Livezey (1987) North Atlantic Oscillation (NAO) during December, January, and February; and the southern nodes agree reasonably well during December and February, but less so during January. Using their centres of action, correlations to snow extent are significantly lower than using ours (Table X), except in February, when the centres of action defined in the two reports are closest. Gutzler and Rosen (1992) also found a correlation of $r = 0.5$ during February between eastern North American snow extent and the NAO, but during December and January they found no significant correlation. The centres of action of Wallace and Gutzler (1981), defined seasonally, are generally far from those defined in this report, and correlations between eastern snow extent and their index tend to be poor (Table X). During March, when

snow extent is effectively decoupled from remote tropospheric fluctuations, teleconnection indices are uncorrelated to snow extent regardless of how the nodes are defined.

7. SUMMARY AND CONCLUSIONS

In this analysis we have examined the kinematics of snow extent fluctuations across Northern Hemisphere lands at regional to hemispheric scales. During each month from September through June, areas of active snow fluctuations, over which snow cover is ephemeral, cover between 11% and 28% of the land area north of 20°N. The largest active areas occur during October and November, when snow is accumulating over large portions of the continents. Between December and March, active areas are generally located south of 47°N, except for parts of the North American prairies and northern Europe.

Interannual fluctuations of North American and Eurasian snow extents are driven by both hemispheric scale signals, and signals from smaller 'coherent' regions, within which interannual fluctuations of snow extent are highly correlated. Between one and four coherent regions over North America, and two and six over Eurasia, are identified each month. These regions cover only 2–6% of the continental land area north of 20°N, yet during many months explain more than 60% of the variance in continental snow extent, especially over North America. Significant month-to-month persistence in the snow extent signal is found over western North America and Europe during winter and spring.

Geographically and seasonally dependent associations are identified between North American snow extent and 500-mb circulation patterns, surface air temperatures, and snowfall. Over western North America, extensive snow cover is associated with a westward shift by 20–30° longitude of the North American ridge. A teleconnection index associated with ridge location is defined. This Western North American Snow Index has two nodes: one over the western land mass, and one over the eastern North Pacific Ocean. Over eastern North America, snow extent is associated with a dipolar oscillation in the 500-mb geopotential height field. The Eastern North American Snow Index, which is significantly correlated to eastern North American snow extent, has one node over southern Greenland and one over the mid-latitude North Atlantic Ocean. These indices represent secondary modes of variability in tropospheric circulation that are not captured by EOF analyses of geopotential heights.

During spring, snow extent becomes effectively decoupled from tropospheric dynamics. Correlations between regional snow extent and snow indices are insignificant during March and April. However, significant correlations are maintained between snow extent and surface temperatures, and snow extent and 500-mb heights directly above the region. Evidence suggests that snow extent is more than a passive product of circulation regimes: the presence of snow exerts an influence on lower tropospheric temperatures that can, through a series of feedbacks, modulate atmospheric circulation patterns. However, quantification of these feedbacks is beyond the scope of this analysis.

These results are important for understanding the natural variability of the climate system. Current generation climate models are able to reproduce mean annual snow extent with considerable accuracy. However, the seasonal and spatial distributions of snow extent are less accurately represented, interannual variability is underestimated, and models are inconsistent in capturing the circulation associations identified here (Frei, 1997; Frei and Robinson, 1998). Currently, efforts are underway to investigate in more detail these relationships using both observations and models, in order to understand the interactions between snow cover and tropospheric dynamics, and to evaluate models.

The identification of coherent regions allows us to reconstruct pre-satellite era snow extent using historical station observations. By taking advantage of the well-defined geographical boundaries of coherent regions identified in this report, snow depth observations can be used to estimate regional and continental snow extent, even in regions with sparse station distributions. In a companion paper to this (Frei *et al*., 1999), historical fluctuations of North American snow extent are recreated back to 1900, more than tripling the satellite-derived record length of approximately 25 years. A similar analysis is planned for Eurasia, where station observations of snow depth from the former Soviet Union and China have recently been made available.

These efforts are directed towards the ultimate goal of using snow observations to detect climate change using a pattern-based, or 'fingerprint' approach. As outlined by a panel convened by the US Department of Energy (Pennell *et al*., 1993), there are two priorities for such approaches. One is to estimate the natural variability. The second is to determine the feasibility of attributing observed changes to known causes. Climate models are required for this task, and must be evaluated in more detail if we are to have confidence in predictions of snow extent under altered climatic conditions.

ACKNOWLEDGEMENTS

AF performed this work under a NASA Graduate Student Fellowship in Global Change Research in the Department of Geography, Rutgers University, and as a Visiting Scientist at the National Snow and Ice Data Center, University of Colorado; DAR is supported by NSF grants ATM-9314721 and SBR-9320786, and NASA grant NAGW-3586. We thank Don Garrett at the NOAA Climate Analysis Center for providing satellite data; thanks also to Robert Livezey and one anonymous reviewer for helpful comments.

REFERENCES

Baker, D.G., Ruschy, D.L., Skaggs, R.H. and Wall, D.B. 1992. 'Air temperature and radiation depressions associated with a snow cover', *J. Appl. Met*., **31**, 247–254.

Barnett, T.P., Dumenil, L., Schlese, U., Roeckner, E. and Latif, M. 1989. 'The effect of Eurasian snow cover on regional and global climate model variations', *JAS*, **46**, 661–685.

Barnston, A.G. and Livezey, R.E. 1987. 'Classification, seasonality and persistence of low-frequency atmospheric circulation patterns', *MWR*, **115**, 1083–1126.

Barry, R.G. 1985. 'The cryosphere and climatic change', in MacCracken, M.C. and Luther, F.M. (eds), *Detecting the Climatic Effects of Increasing Carbon Dioxide*, USDOE, Washington DC DOE/ER-0235, pp. 109–148.

Berry, M.O. 1981. 'Snow and climate', in Gray, D.M. and Male, D.H. (eds), *Handbook of Snow: Principles*, *Processes*, *Management* and *Use*, Pergamon Press, Oxford, pp. 32–59.

Brown, R.D. 1995. 'Spatial and temporal variability of North American snow cover, 1971–1992', *Proceedings of the Eastern Snow Conference*, *52nd Annual Meeting*, *June 6–8 1995*, Toronto, Ontario, pp. 69–78.

Brown, R.D. 1997. 'Historical variability in Northern Hemisphere spring snow covered area', *Ann. Glac*., **25**, 340–346.

Brown, R.D. and Goodison, B.E. 1996. 'Interannual variability in reconstructed Canadian snow cover, 1915–1992', *J. Clim*., **9**, 1299–1318.

Cerveny, R.S. and Balling, R.C. Jr. 1992. 'The impact of snow cover on diurnal temperature range', *GRL*, **19**, 797–800.

Chang, A.T.C., Foster, J.L. and Hall, D.K. 1990. 'Satellite sensor estimates of Northern Hemisphere snow volume', *Int. J. Rem. Sens*., **11**, 167–171.

Clark, M.P. 1998. *The Role of Snow Cover in the Climate System*, PhD Dissertation, University of Colorado, Boulder, CO.

Clark, M.P. and Serreze, M.C. 1999a. 'Influence of variability in East Asian snow cover on atmospheric circulation over the North Pacific Ocean', *Extended Abstracts from the 95th Conference on Polar Meteorology And Oceanography*, Dallas, TX, 11–15 January, J7.6, American Meteorological Society, Boston, MA, 261–266.

Clark, M.P. and Serreze, M.C. 1999b. 'Snowfall responses over the U.S.A. to phase and amplitude variations in the tropospheric wavetrain', *Proceedings of the IAHS*, Birmingham, UK, September, in press.

Clark, M.P., Serreze, M.C. and Robinson, D.A. 1999. 'Atmospheric controls on Eurasian snow extent', *Int. J. Climatol*., **19**, 27–40.

Dewey, K.F. 1977. 'Daily maximum and minimum temperature forecasts and the influence of snow cover', *MWR*, **105**, 1594–1597.

Dewey, K.F. and Heim, R. Jr. 1982. 'A digital archive of Northern Hemisphere snow cover, November 1966 through December 1980', *BAMS*, **63**, 1132–1141.

Dey, B. and Bhanu Kumar, O. 1983. 'Himalayan winter snow cover area and summer monsoon rainfall over India', *JGR*, **88**(C9), 5471–5474.

Dey, B., Kathuria, N. and Bhanu Kumar, O. 1985. 'Himalayan summer snow cover and withdrawal of the Indian summer monsoon', *J. Clim. Appl. Met*., **24**, 865–868.

Dickson, R.R. and Namias, J. 1976. 'North American influences on the circulation and climate of the North Atlantic sector', *MWR*, **104**, 1255–1265.

Foster, J., Owe, M. and Rango, A. 1983. 'Snow cover and temperature relationships in North America and Eurasia', *J. Clim. Appl. Met*., **22**, 460–469.

Frei, A. 1997. *Towards a Snow Cover Fingerprint for Climate Change Detection*. PhD Dissertation submitted to the Graduate School—New Brunswick, Rutgers, The State University of New Jersey, USA.

Frei, A. and Robinson, D.A. 1998. 'Evaluation of snow extent and its variability in the atmospheric model intercomparison project', *JGR-Atmospheres*, **103**(D8), 8859–8871.

Frei, A., Hughes, M.G., and Robinson, D.A. 1999. 'North American snow extent: 1910–1994', *Int. J. Climatol*., **19**, 1517–1534.

Groisman, P.Ya., Karl, T.R. and Knight R.W. 1994a. 'Observed impact of snow cover on the heat balance and the rise of continental spring temperatures', *Science*, **263**, 198–200.

Groisman, P.Ya., Karl, T.R., Knight, R.W. and Stenchikov, G.L. 1994b. 'Changes of snow cover, temperature, and radiative heat balance over the Northern Hemisphere', *J. Clim.*, **7**(11), 1633–1656.
Gutzler, D.S. and Rosen, R.D. 1992. 'Interarmual variability of wintertime snow cover across the Northern Hemisphere', *J. Clim.*, **5**, 1441–1447.
Hahn, D.G., and Shukla, J. 1976. 'An apparent relationship between Eurasian snow cover and Indian monsoon rainfall', *JAS*, **33**, 2461–2462.
Harman, J.R. 1991. *Synoptic Climatology of the Westerlies: Process and Patterns*, Washington, DC, Association of American Geographers, 80 pp.
Harrington, J.A. Jr., Cerveny, R.S. and Dewey, K.F. 1987. 'A climatology of mean monthly snowfall for the conterminous United States: temporal and spatial patterns', *J. Clim. Appl. Met.*, **26**, 897–912.
Heim, R. Jr. and Dewey, K.F. 1984. 'Circulation patterns and temperature fields associated with extensive snow cover on the North American continent', *Phys. Geog.*, **4**, 66–85.
Horel, J.D. 1981. 'A rotated Principal Component Analysis of the interannual variability of the Northern Hemisphere 500-mb height field', *MWR*, **109**, 2080–2092.
Iwasaki, T. 1991. 'Year-to-year variation of snow cover area in the Northern Hemisphere', *J. Meteor. Soc. Jpn.*, **69**, 209–217.
Karl, T.R., Groisman, P.Ya., Knight, R.W. and Heim, R. Jr. 1993. 'Recent variations of snow cover and snowfall in North America and their relation to precipitation and temperature variations', *J. Clim.*, **6**, 1327–1344.
Kocin and Uccellini. 1990. 'Snowstorms along the northeastern coast of the United States: 1955 to 1985', *American Meteorological Society*, *Meteorol. Monogr.*, **22** (44), 280.
Kukla, G. and Robinson, D.A. 1981. 'Accuracy of operational snow and ice charts', *1981 IEEE International Geoscience and Remote Sensing Symposium Digest*, 974–987.
Leathers, D.J. and Palecki, M.A. 1992. 'The Pacific/North American teleconnection pattern and United States climate. Part II: temporal characteristics and index specification', *J. Clim.*, **5**, 707–716.
Leathers, D.J. and Robinson, D.A. 1993. 'The association between extremes in North American snow cover extent and United States temperatures', *J. Clim.*, **6**, 1345–1355.
Leathers, D.J. and Robinson, D.A. 1997. 'Abrupt changes in the seasonal cycle of North American snow cover', *J. Clim.*, **10** (10), 2569–2585.
Leathers, D.J., Yarnal, B., and Palecki, M.A. 1991. 'The Pacific/North American teleconnection pattern and United States climate. Part I: regional temperature and precipitation associations', *J. Clim.*, **4**, 517–528.
Leathers, D.J., Mote, T.L., Kuivinen, K.C., McFeeters, S. and Kluck, D.R. 1993. 'Temporal characteristics of USA snowfall 1945–1946 through to 1984–1985', *Int. J. Climatol.*, **13**, 65–76.
Leathers, D.J., Ellis, A.W. and Robinson, D.A. 1995. 'Characteristics of temperature depressions associated with snow cover across the northeast United States', *J. Appl. Met.*, **34**, 381–390.
Livezey, R.E. and Chen, W.Y. 1983. 'Statistical field significance and its determination by monte carlo techniques', *MWR*, **111**, 46–59.
Livezey, R.E. 1995. 'The evaluation of forecasts', in H. von Storch and A. Navarra (eds), *Analysis of Climate Variability: Applications of Statistical Techniques* (Chapter 10), Springer Verlag, Berlin, p. 194.
Masuda, K., Morinaga, Y., Numaguti, A. and Abe-Ouchi, A. 1993. *The Annual Cycle of Snow Cover Extent over the* Northern Hemisphere *as Revealed by NOAA/NESDIS Satellite Data*, Geographical Reports of Tokyo Metropolitan University # 28, 113–132.
Matson, M., Ropelewski, C.F. and Varnadore, M.S. 1986. *An Atlas of Satellite-derived Northern Hemispheric Snow Cover Frequency*, NOAA Atlas, National Oceanic and Atmospheric Administration, 75 pp.
Namias, J. 1985. 'Some empirical evidence for the influence of snow cover on temperature end precipitation', *MWR*, **113**, 1542–1553.
O'Lenic, E.A. and Livezey, R.E. 1988. 'Practical considerations in the use of rotated principal component analysis (RPCA) in diagnostic studies of upper-air height fields', *MWR*, **116**, 1682–1689.
Pennell, W.T., Barnett, T.P., Hasselmann, K., Holland, W.R., Karl, T.R., North, G.K., MacCracken, M.C., Moss, G., Pearman, E.M., Rasmusson, B.D., Santer, D.D., Smith, W.K., von Storch, H., Switzer, P. and Zweirs, F. 1993. 'The detection of anthropogenic climate change', *Proceedings of the Fourth Symposium on Global Change Studies*, American Meteorological Society, Anaheim, CA, pp. 21–27.
Robinson, D.A. 1993a. 'Hemispheric snow cover from satellites', *Ann. Glac.*, **17**, 367–371.
Robinson, D.A. 1993b. 'Global snow cover monitoring: an update', *BAMS*, **74**(9), 1689–1696.
Robinson, D.A. 1993c. 'Historical daily climatic data for the United States', *Proceedings of the Eighth Conference on Applied Climatology*, American Meteorological Society, Anaheim, CA, pp. 264–269.
Robinson, D.A. 1999. 'Northern Hemisphere snow extent during the satellite era', *Preprints: Fifth Conference on Polar Meteorology and Oceanography*, *Dallas*, *TX*, American Meteorological Society, pp. 255–258.
Robinson, D.A., Keiming, F.T. and Dewey, K.F. 1991. 'Recent variations in Northern Hemisphere snow cover', *Proceedings of the 15th Annual Climate Diagnostics Workshop*, NOAA, Washington, DC, pp. 219–224.
Robinson, D.A., Frei, A. and Serreze, M.C. 1995. 'Recent variations and regional relationships in Northern Hemisphere snow cover', *Ann. Glac.*, **21**, 71–76.
Robinson, D.A. and Frei, A. 1997. 'A Northern Hemisphere snow cover climatology using satellite information', *Proceedings of the 10th conference on Applied Climatology*, *American Meteorological Society*, Reno, NV, pp. 24–28.
Robinson, D.A. and Leathers, D.J. 1993. 'Associations between snow cover extent and surface air temperature over North America', *Proceedings of the 50th Eastern Snow Conference*, Quebec City, Que, pp. 189–196.
Ross, B. and Walsh, J.E. 1986. 'Synoptic-scale influences of snow cover and sea ice', *MWR*, **114**, 1795–1810.
Sankar-Rao, M., Lau, K.M. and Yang, S. 1996. 'On the relationship between Eurasian snow cover and the Asian summer monsoon', *Int. J. Clim.*, **16**, 605–616.

Serreze, M.C., Rogers, J.C., Carse, F. and Barry, R.G. 1996. 'Icelandic low cyclone activity: climatological features, linkages with the NAO and relationships with recent changes in the Northern Hemisphere circulation', *J. Clim.*, **10**, 453–464.
Serreze, M.C., Clark, M.P., McGinnis, D.L. and Robinson, D.A. 1998. 'Characteristics of snowfall over the eastern half of the United States and relationships with principal modes of low-frequency atmospheric variability', *J. Clim.*, **11**, 234–249.
Shine, K.P., Derwent, R.G., Wuebbles, D.J. and Morcrette, J. 1990. 'Radiative forcing of climate', in Houghton, J.T., Jenkins, G.J. and Ephraums, J.J. (eds), *Climate Change: the IPCC Scientific Assessment*, Cambridge University Press, Cambridge, pp. 41–68.
Steppuhn, H, 1981. 'Snow and agriculture', in Gray, D.M. and Male, D.H. (eds), *Handbook of Snow: Principles*, *Processes*, *Management* and *Use*, Pergamon Press, Oxford, pp. 60–126.
van Loon, H. and Rogers, J.C. 1978. 'The seesaw in winter temperatures between Greenland and northern Europe. Part I: general description', *MWR*, **106**, 296–310.
Wagner, A.J. 1973. 'The influence of average snow depth on monthly mean temperature anomaly', *MWR*, **101**, 624–626.
Wallace, J.M. and Gutzler, D.S. 1981. 'Teleconnections in the geopotential height field during the Northern Hemisphere winter', *MWR*, **109**, 784–812.
Walsh, J.E. 1995. 'Long-term observations for monitoring of the cryosphere', *Clim. Change*, **31**, 369–384.
Walsh, J.E., Tucek, D.R. and Peterson, M.R. 1982. 'Seasonal snow cover and short-term climatic fluctuations of the United States', *MWR*, **110**, 1474–1485.
Walsh, J.E., Jasperson W.H., and Ross, B. 1985. 'Influences of snow cover and soil moisture on monthly air temperatures', *MWR*, **113**, 756–768.
Whittaker, L.M. and Horn, L.H. 1981. 'Geographical and seasonal distribution of North American cyclogenesis, 1958–1977', *MWR*, **109**, 2312–2322.
Wiesnet, D.R., Ropelewski, C.F., Kukla, G.J. and Robinson, D.A. 1987. 'A discussion of the accuracy of NOAA satellite-derived global seasonal snow cover measurements', *Large Scale Effects of Seasonal Snow Cover*, *Proceedings of the Vancouver Symposium*, *August 1987*, Vancouver, IAHS Publ. no. 166, pp. 291–304.
Yang, S. 1996. 'ENSO–snow–monsoon associations and seasonal-interannual predictions', *Int. J. Clim.*, **16**, 125–134.

